文章编号：1001-9014(2023)04-0483-07

DOI：10. 11972/j. issn. 1001-9014. 2023. 04. 009

High-efficiency AlN/GaN MIS-HEMTs with SiN_x insulator grown in-situ for millimeter wave applications

CHEN Xiao-Juan[1,2*], ZHANG Yi-Chuan[2], ZHANG Shen[2], LI Yan-Kui[2], NIU Jie-Bin[2], HUANG Sen[2], MA Xiao-Hua[1], ZHANG Jin-Cheng[1], WEI Ke[2*]

(1. Xidian University, Xi'an 710071, China;
2. Institute of Microelectronics, Chinese Academy of Sciences, Beijing 100029, China)

Abstract: In this work, high-efficiency AlN/GaN metal-insulator-semiconductor high electron mobility transistors (MIS-HEMTs) have been fabricated for millimeter wave applications. A 5-nm SiN_x insulator is grown in-situ as the gate insulator by metal-organic chemical vapor deposition (MOCVD), contributing to remarkably suppressed gate leakage, interface state density and current collapse. The fabricated MIS-HEMTs exhibit a maximum drain current of 2. 2 A/mm at V_{GS}=2 V, an extrinsic peak G_m of 509 mS/mm, and a reverse Schottky gate leakage current of 4. 7×10^{-6} A/mm when V_{GS} = -30 V. Based on a 0. 15 μm T-shaped gate technology, an f_T of 98 GHz and f_{MAX} of 165 GHz were obtained on the SiN/AlN/GaN MIS-HEMTs. Large signal measurement shows that, in a continuous-wave mode, the MIS-HEMTs deliver an output power density (P_{out}) of 2. 3 W/mm associated with a power-added efficiency (PAE) of 45. 2% at 40 GHz, and a P_{out} (PAE) of 5. 2 W/mm (42. 2%) when V_{DS} was further increased to 15 V.

Key words: AlN/GaN, metal-insulator-semiconductor High Electron Mobility Transistors (MIS-HEMTs), millimeter wave, low dispersion, low drain voltage

带有原位生长SiN_x绝缘层的AlN/GaN毫米波高效率MIS-HEMT器件

陈晓娟[1,2*]，张一川[2]，张 昇[2]，李艳奎[2]，牛洁斌[2]，黄 森[2]，
马晓华[1]，张进成[1]，魏 珂[2*]

(1. 西安电子科技大学,陕西 西安 710071;
2. 中国科学院微电子研究所,北京 100029)

摘要:本文采用金属有机化学气相沉积(MOCVD)生长原位SiNx栅介质制备了用于Ka波段高功率毫米波应用的AlN/GaN金属绝缘体半导体高电子迁移率晶体管(MIS-HEMTs)。原位生长SiN_x栅介质显著抑制了栅反向漏电、栅介质/AlN界面态密度和电流坍塌。所研制的MIS HEMTs在V_{GS}= 2 V时最大饱和输出电流为2.2 A/mm,峰值跨导为509 mS/mm,在V_{GS}= -30 V时肖特基栅漏电流为4.7×10^{-6} A/mm。采用0.15 μmT形栅技术,获得98 GHz的f_T和165 GHz的f_{MAX}。大信号测量表明,在连续波模式下,漏极电压V_{DS}= 8 V时,MIS HEMT在40 GHz下输出功率密度2.3 W/mm,45.2%的功率附加效率(PAE),而当V_{DS}增加到15 V时,功率密度提升到5.2 W/mm,PAE为42.2%。

关 键 词:AlN/GaN;金属绝缘体半导体高电子迁移率晶体管;Ka波段;低损耗;低偏压

中图分类号:O48　　**文献标识码**:A

Received date: 2022- 06- 22, **revised date**: 2022- 11- 02　　**收稿日期**:2022- 06- 22,**修回日期**:2022- 11- 02

Foundation items: Supported by the National Natural Science Foundation of China (61822407, 62074161, 62004213); the National Key Research and Development Program of China under (2018YFE0125700)

Biography: CHEN Xiao-Juan (1979-), female, ChongQing, master. Research area involves Compound Semiconductor materials and devices. E-mail: chenxiaojuan@ime. ac. cn.

* **Corresponding authors**: E-mail: chenxiaojuan@ime. ac. cn, weike@ime. ac. cn

Introduction

In recent years, high electron mobility transistors (HEMTs) based on GaN have attracted more attention, due to their high thermal conductivity, high breakdown voltage, and high-power density for millimeter-wave (mm-wave) power amplifiers. In an AlGaN/GaN HEMTs structure, the working voltage may reach 28 V or even higher[1][2], such high voltage will enhance the longitudinal electric field to increase the gate leakage[3]. Additionally, the internal electric field intensity will reach 10^6~10^7 V/cm when the 20~30 V is applied to drain bias, leading to current collapse, reduction of breakdown voltage, and increase in leakage[4]. In order to achieve high-performance GaN HEMT at low operating voltage, the energy-band theory is used to design new epitaxial structures to increase the electron gas density meanwhile preventing the gate from losing its control ability for the short T-gate. Therefore, the ultra-thin barrier layer technology has shown great advantages in ultra-high frequency and high power[5][6].

In millimeter-wave applications, the gate length is shrunk to deep-submicron size, and the transverse dimension of the device needs to be scaled down at the same proportion. To avoid the short channel effect, the material structure with an ultra-thin barrier layer is used to solve the aspect ratio of the gate. The issue primarily results from the much stronger spontaneous and piezoelectric polarization of AlN/GaN compared to AlGaN/GaN, leading to a much higher drain current in the HEMT channel, also allowing the use of a much thinner barrier layer. While along with the shrink of vertical device dimensions, increased gate leakage necessitates the use of a gate insulator[7-10].

AlN barrier has been shown highly sensitive to the air and vapor for oxidation, consequently, surface treatment and passivation techniques play a significant role in the surface state. To achieve a low gate leakage current, materials with a wide bandgap are necessary, such as SiO_2 and Al_2O_3[7][9]. However, it is inevitable that these materials are deposited on the AlN surface when it is exposed to air, becoming contamination at the interfaces. On the other hand, in-situ deposition of SiN_x is a promising way to realize proper interfaces, which guarantees the insensitivity of AlN surfaces to temperature change.

In this work, we demonstrated the AlN/ GaN MIS-HEMTs. By using in-situ SiN_x insulator, a maximum drain current $I_{D,max}$ of 2.2 A/mm was obtained at V_{GS}=2 V, it doubled $I_{D,max}$ of the AlGaN/GaN HEMTs under the same condition. Transconductance $G_{m,ext}$ of 509 mS/mm are also achieved. Moreover, the OFF-state drain leakage, as well as gate leakage current in the HEMTs, was reduced by the low interface state between AlN barrier and insulator, contributing to a low Schottky gate leakage of 4.7×10^{-6} A/mm at V_{GS} = -30 V and a low OFF-state drain leakage of 8.2×10^{-5} A/mm. Owing to the suppressed current collapse, when V_{DS} = 8 V, a high output power density of 2.3 W/mm with peak power-added-efficiency (PAE) of 45.2%, and a power gain of 10.2 dB are achieved at 40 GHz in the continuous-wave (CW) mode.

1 Experiments

The schematic cross section of MIS-HEMTs is shown in Fig. 1(a). The AlN/GaN heterostructures in this study were grown on semi-insulating SiC substrates by metal-organic chemical vapor deposition (MOCVD), consisting of a Fe-doped GaN buffer layer, an unintentionally doped GaN channel layer, 1 nm AlN spacer layer, a 5 nm AlN barrier layer, and 5 nm SiN_x insulator layer. Device fabrication was started with source/drain ohmic contact formation by Ti/Al/Ni/Au stack, and subsequent rapid thermal annealed at 800 ℃ for 30 s in N_2 atmosphere, to yield a contact resistance of 0.3 Ω·mm. Device isolation was then formed utilizing multiple-energy nitrogen ion implantation. A T-shaped gate was subsequently accomplished by electron beam lithography (EBL; model manufacturer) of UVIII/Al/PMMA resist stack. The width of the T-gate foot and head are 0.15 and 0.6 μm, respectively[2]. A Ni/Au metal layer was generated by e-beam evaporation (EVA450) on SiN_x's surface for the gate contact. Finally, the AlN/GaN HEMT devices were passivated with 60 nm stress-free SiN_x grown by plasma-enhanced chemical vapor deposition (PECVD). The fabricated MIS-HEMTs

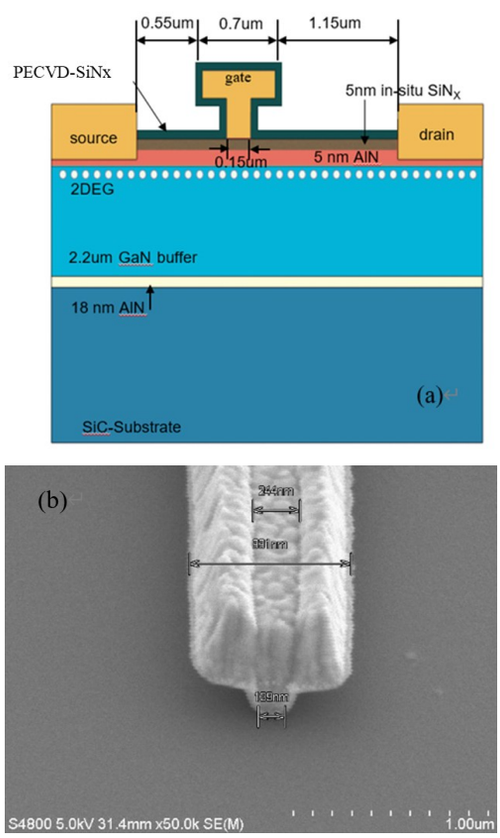

Fig.1 (a) The schematic of epitaxial structure of AlN/GaN MIS-HEMTs, (b) the SEM of 0.15-μm T-gate
图1 (a)外延材料与器件结构示意图,(b)0.15 μmT型栅扫描电镜图

have a source-drain distance (L_{SD}) of 2.4 μm and a gate-drain distance (L_{GD}) of 1.15 μm. An SEM picture of the T-gate is shown in Fig. 1(b).

As a comparison, AlGaN/GaN HEMT devices are also developed, with the barrier and cap layers replaced with a 21-nm $Al_{0.25}Ga_{0.75}N$ and a 3-nm GaN layers, respectively, as Ref. [16]. The gate recessed process, which differs from the AlN/GaN device's, uses inductively coupled plasma (ICP) dry etching with chlorine-based plasmas of BCl_3 and Cl_2 to fabricate recessed-gate with a width of 0.8 μm and depth of 6 nm. Then the same T-shaped gates were fabricated on it. The remaining process steps are the same as for AlN/GaN devices.

2 Results and discussions

2.1 DC measurement

The fabricated devices yielded in this study exhibit a typical static characterization, as shown in Fig. 2(a). Due to the much stronger spontaneous and piezoelectric polarization of AlN/GaN, a maximum drain current of 2.2 A/mm at V_{GS}=2 V was observed. The thickness of the in-situ SiN_x cap layer is critical for highly scaled GaN devices to avoid gate leakage current contributing to a reverse density of 4.7×10^{-6} A/mm at V_{GS} = -30 V, as shown in Fig. 2(b). The short-channel effect was effectively suppressed

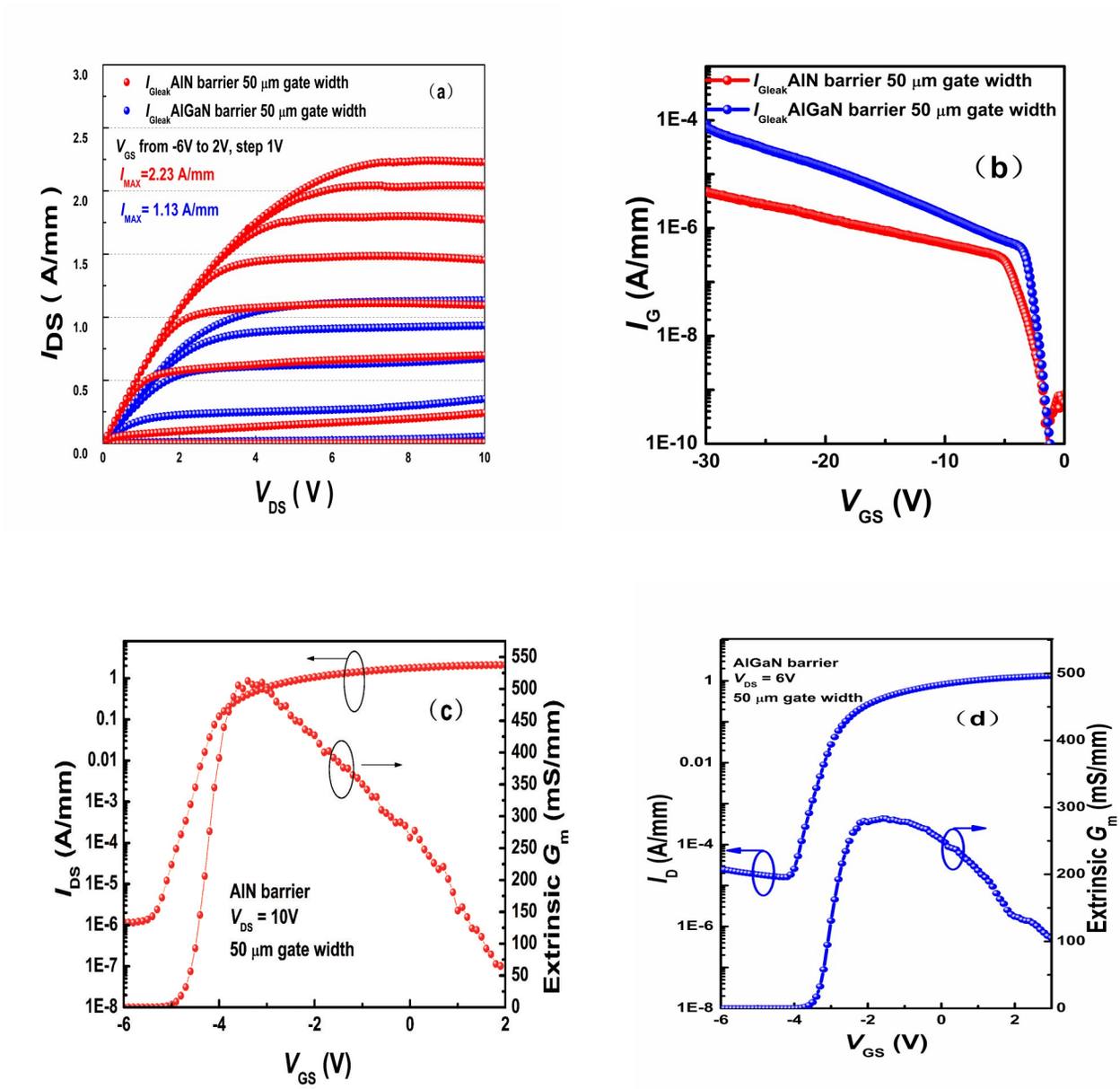

Fig. 2 Measured dc characteristics of devices (a) I_D of both HEMTs and MIS-HEMTs versus V_{DS} with V_{GS} varied from -6 V to 2 V, (b) gate leakage of HEMTs and MIS-HEMTs with V_{GS} swept to -30 V, (c) I_D and extrinsic transconductance of MIS-HEMTs with V_{GS} varied from -6 V to 2 V at V_{DS}= 6 V, (d) I_D and extrinsic transconductance of HEMTs with V_{GS} varied from -6 V to 3 V at V_{DS}= 6 V

图2 器件直流特性测试(a) HEMT和MIS-HEMT器件输出电流特性测试对比图,(b) HEMT和MIS-HEMT器件肖特基特性测试对比图,(c)MIS-HEMT器件转移特性测试图,(d)HEMT器件转移特性测试图

by the thin barrier, as shown by the transfer curves in Fig. 2(c), and the OFF-state drain leakage is merely 1.0×10^{-6} A/mm. Meanwhile the corresponding $G_{m,ext}$ at V_{DS} = 6 V is 509 mS/mm (Fig. 2(c)). Based on AlGaN barrier device, $G_{m,ext}$ is 294 mS/mm and the OFF-state drain leakage is 8.2×10^{-5} A/mm under the same test condition (Fig. 2(d)).

2.2 The small-signal RF characteristics

The small-signal RF characteristics of the fabricated MIS-HEMTs were measured using a network analyzer in a frequency range from 100 MHz to 40 GHz. Values of current-gain cutoff frequency f_T and unit-power-gain frequency f_{MAX}, as shown in Fig. 4, were determined by 20 dB/dec line extrapolated from the small-signal current gain |h21|and maximum stable gain (MSG). At V_{DS}=10 V, f_T and f_{MAX} are 98 GHz and 165 GHz, respectively (Fig. 3). It implies that in-situ SiN_x technology effectively suppresses the RF-G_m collapse in mm-wave AlN/GaN HEMTs.

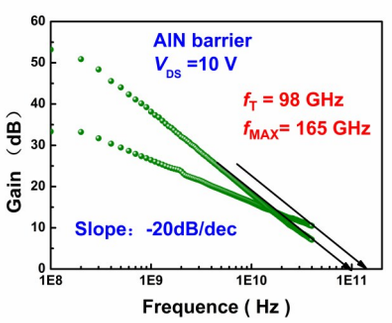

Fig. 3 Small-signal characteristics of the fabricated AlN/GaN MIS-HEMTs at V_{DS} = 10 V
图3 VDS = 10 V下AlN/GaN MIS-HEMTs器件小信号测试图

2.3 CV and pulse measurement

To determine the quality of in-situ SiN_x, the capacitance-voltage(C-V) measurement was employed to realize interface trap density. The frequency/temperature dispersions of the second slope in C-V curve were analyzed[11-13], and the results are shown in Fig. 4. With f_m varying from 1 KHz to 1 MHz (Fig. 4(a)), and T increasing from 25 ℃ to 150 ℃ (Fig. 4(b)), the C-V characteristics of AlN/GaN MIS-HEMT exhibits a slight (ΔV less than 0.05 V) dispersions in multi-f/T ac-CV characteristics, indicating low Dit and high interface quality in MIS-HEMT. Accordingly, D_{it} at the in-situ SiN_x/AlN interface was mapped against E_T[14-15]. From E_C-0.58 eV to E_C -0.29 eV, D_{it} falls between 3.4×10^{11} and 1.1×10^{12} $cm^{-2}eV^{-1}$ (Fig. 4(c)).

The low interface state density ensures the low dc-RF dispersion, the pulse I-V characteristic of the devices is shown in Fig. 5(a). The pulse period and width were set to 10 μs and 200 ns, respectively. The gate-lag effect under a quiescent bias of (V_{GSQ}, V_{DSQ}) = (-6 V, 0 V) barely changes in the MIS-HEMTs. The drain-lag ratio under a quiescent bias of (V_{GSQ}, V_{DSQ}) = (-6 V, 15 V) is pretty weak in the saturation region (collapse ratio: 1.5%, Fig. 5(a)). It is probably due to the N in the SiN_x rather than

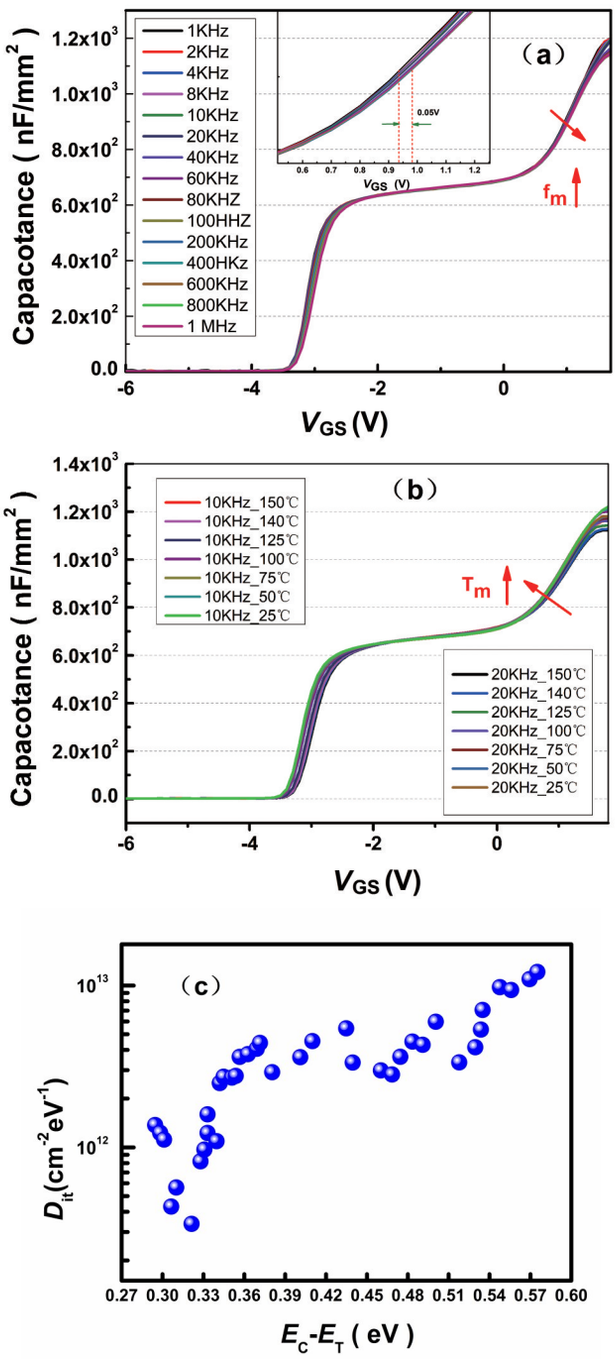

Fig. 4 f/T-dependent C-V characteristics of AlN/GaN MIS-HEMTs with (a) f_m varying from 1 KHz to 1 MHz, (b) T increasing from -25 ℃ to 150 ℃ f_m varying at 10 KHz and 20 KHz (c) D_{it}-E_T mapping in AlN/GaN MIS-HEMTs
图4 (a)AlN/GaN MIS-HEMTs不同频率下的CV测试图,(b)频率10 HKz和20 KHz下AlN/GaN MIS-HEMTs从-25到150 ℃的CV特性测试图,(c)AlN/GaN MIS-HEMTs多频-变温下计算的Dit-ET关系图

the AlN barrier that leads N vacancies creating a conducting channel through the AlN barrier, hence low annealing temperature and time. The in-situ SiN_x impeded the formation of nitrogen deficiency and oxidation of bare AlN surface when conventional process of ohmic annealing at above 800 ℃, and suppressed damage to the AlN barrier

during the process of extra SiN_X ex-situ passivation. The ultralow dispersion implies that in-situ SiN_X effectively obstructed the bombardment of ion when the plasm was generated. As shown the pulsed transfer characteristics curves in Fig. 5(b), hysteresis is less than 100 mV after sweeping from -8 V to 0 V, indicating significant suppression of deep interface traps with in-situ insulator.

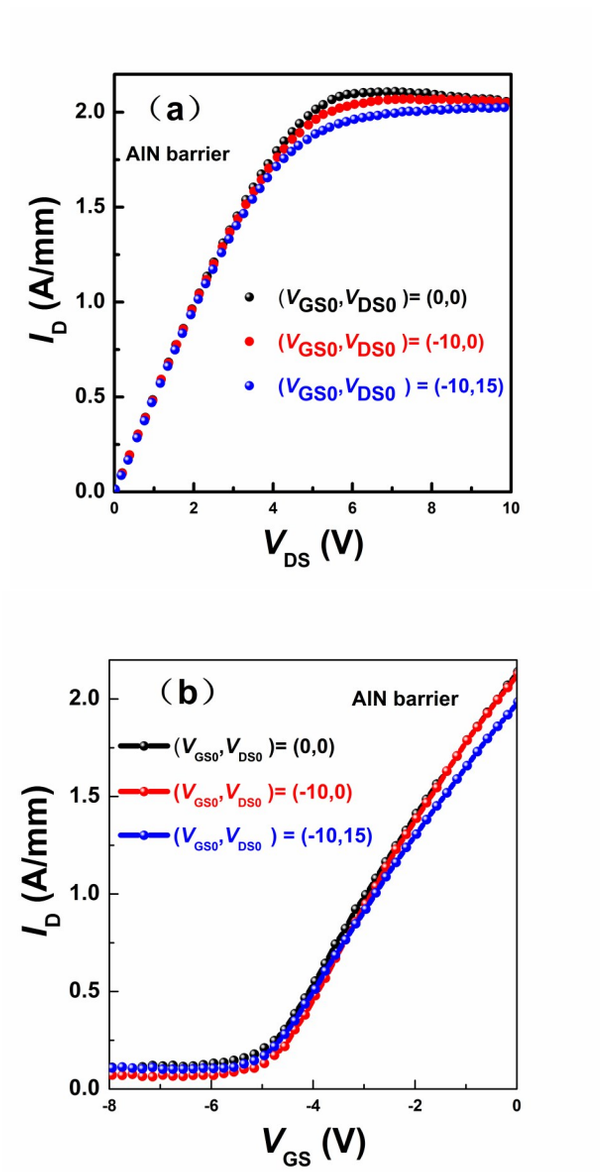

Fig. 5 Pulsed I-V characteristics of (a) output characteristics measured at V_{GS} = 0 V, (b) transfer characteristics measured at V_{DS} = 10 V

图5 脉冲测试图(a)VGS = 0 V下,不同静态偏置下饱和输出电流测试对比图,(b)VDS = 10 V时不同静态偏置下转移特性对比测试图

2.4 Large-signal measurement

Figure. 6 depicts the large-signal power performance of the mm-wave AlN/GaN MIS-HEMTs, evaluated at 40 GHz in CW mode, in comparison with AlGaN/GaN HEMTs. The devices were biased at Class-AB condition with low operation voltage, V_{DS} = 8 V, V_{DS} = 10 V, and V_{DS} = 15 V, respectively. Load and source impedance were optimized for the best PAE before the evaluation.

Owing to the enlarged current density and minimized forward gate leakage current of AlN/GaN MIS-HEMTs, a record high PAE of 45.2% is achieved at V_{DS} = 8 V, and the corresponding output power density and associated gain are 2.3 W/mm and 10.8 dB gain. By contrast, the PAE, output power density, and gain of AlGaN/GaN HEMTs are merely 42.6%, 1.2 W/mm, and 9.1 dB respectively. when V_{DS} = 10 V, P_{out} of AlN/GaN MIS-HEMTs reached 3.3 W/mm while that of AlGaN/GaN HEMTs is 1.5 W/mm; when V_{DS} = 15 V, P_{out} of AlN/GaN MIS-HEMTs increased to 5.2 W/mm while that of AlGaN/GaN HEMTs is 2.8 W/mm. In previous research using the AlGaN HEMTs structure, P_{out} of 5.1 W/mm can be only obtained under V_{DS} over 25 V[16]. The high performance of AlN/GaN HEMTs is believed to attribute to the wide conduction band between AlN and GaN, as well as the high-quality SiN_x/AlN interface.

At low voltage, the power density of AlN / GaN thin barrier MIS-HEMTs based on in-situ SiN growth is nearly double that of AlGaN barrier devices, making them promising for low voltage applications.

3 Conclusions

With in-situ SiN_x technique on AlN/GaN epi-structure and T-gate process, high-performance MIS-HEMTs have been fabricated for low V_{DS} applications at Ka-band. A high-quality SiN_x/AlN interface has been obtained, which was verified by analyzing the frequency and temperature-dependent of the second slope in the C-V characteristics. Using 0.15 μm Γ-shaped gate technology, the developed MIS-HEMTs show a maximum drain current of 2.2 A/mm at V_{GS}=2 V, an extrinsic peak $G_{m,ext}$ of 509 mS/mm, extra-low dc-RF dispersion. The drain-lag ratio of 1.5% under a quiescent bias of (V_{GSQ}, V_{DSQ}) = (-6 V, 15 V) collapse-ratio in the saturation region. the MIS-HEMTs can yield an output power density of 2.3 W/mm associated with power-added efficiency (PAE) of 45.2% at 40 GHz under the drain voltage V_{DS}=8 V in continuous-wave mode. Furthermore, when V_{DS}=10 V, the power density was 3.3 W/mm, and PAE maintain 43.8%; when V_{DS}= 15 V, power density increased to 5.2 W/mm with PAE decreasing to 42.2%. The results suggest that the in-situ AlN/GaN MIS-HEMTs are promising for low bias voltage applications requiring high-efficiency and high-power density at Millimeter Waves.

References

[1] Moon J S. 55% PAE and high power Ka-band GaN HEMTs with linearized transconductance via n+ GaN source contact ledge[J]. *IEEE Electron Device Lett*, 2008, **29**(8): 834-7.

[2] Zhang Y C, Wei K, Huang S, *et al*. High-Temperature-Recessed Millimeter-Wave AlGaN/GaN HEMTs With 42.8% Power-Added-Efficiency at 35 GHz[J]. *IEEE Electron Device Letters*, 2018. **39**(5): 727-730.

[3] Downey B P, Meyer D J, Katzer D S, *et al*. Effect of SiNx gate insulator thickness on electrical properties of SiNx/In0.17Al0.83N/AlN/GaN MIS-HEMTs[J]. *Solid State Electronics*, 2015, 106(apr.): 12-17.

[4] Gu W P, Duan H T, Ni J Y, *et al*. High-electric-field-stress-induced degradation of SiN passivated AlGaN/GaN high electron mobili-

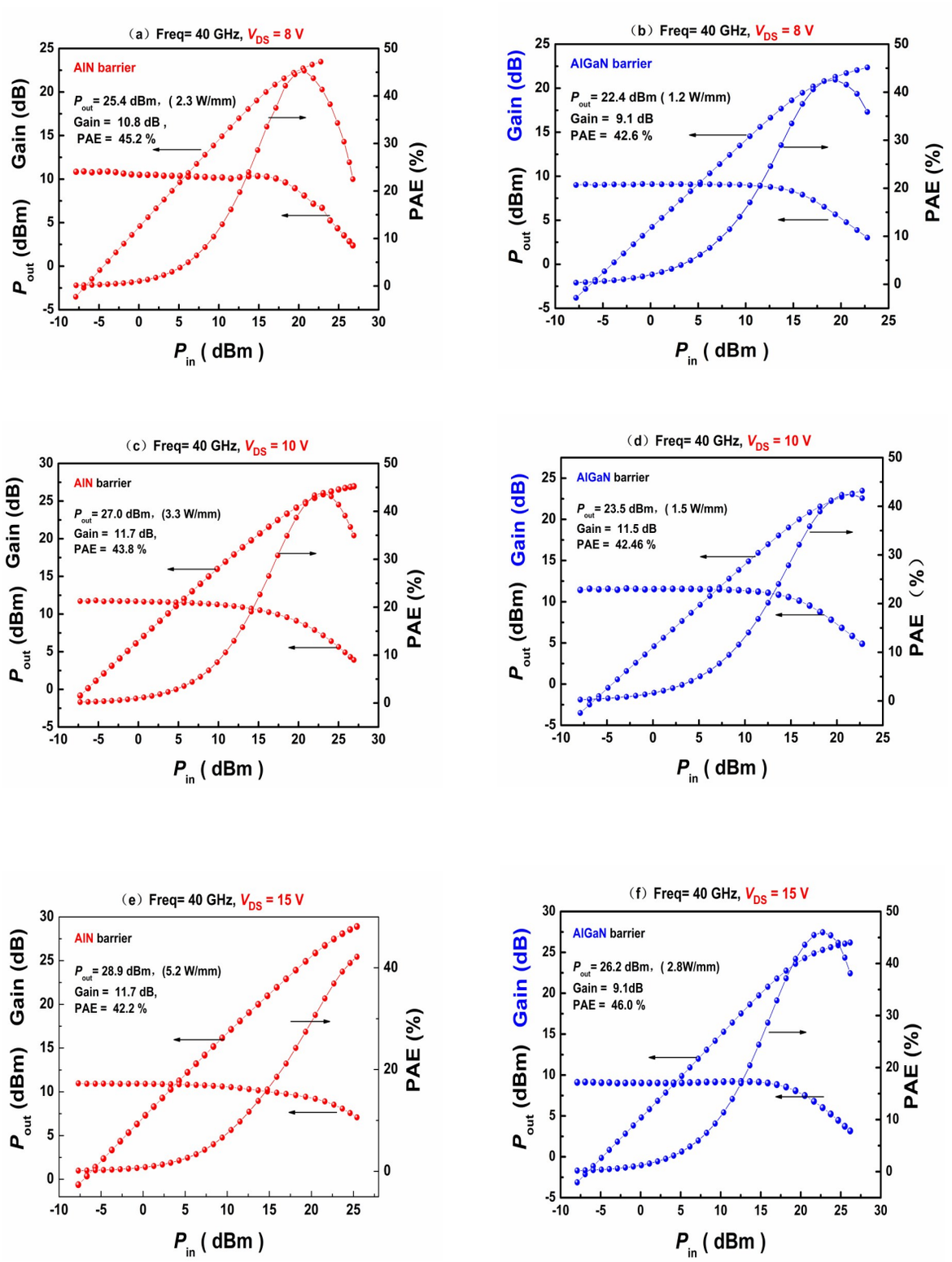

Fig. 6 Large-signal measurements at 40 GHz in CW mode (a) VDS=8 V, AlN/GaN MIS-HEMTs measurement, (b) VDS=8 V, AlGaN/GaN HEMTs measurement, (c) VDS=10 V, AlN/GaN MIS-HEMTs measurement, (d) VDS=10 V, AlGaN/GaN HEMTs measurement, (e) VDS=15 V, AlN/GaN MIS-HEMTs large-signal measurement, (f) VDS=15 V, AlGaN/GaN HEMTs measurement

图6 40 GHz下大信号连续波测试(a)VDS=8 V, AlN/GaN MIS-HEMTs测试结果,(b)VDS=8 V, AlGaN/GaN HEMTs测试结果,(c)VDS=10 V, AlN/GaN MIS-HEMTs测试结果,(d)VDS=8 V, AlGaN/GaN HEMTs测试结果,(e)VDS=15 V, AlN/GaN MIS-HEMTs测试结果,(f)VDS=15 V, AlGaN/GaN HEMTs测试结果

ty transistors SiN passivated AlGaN/GaN high electron mobility transistors [J]. *Chinese Physics B*, 2009, (4): 1601 -1608.
[5] Medjdoub F, Okada E, Grimbert B, *et al*. Towards millimeter-wave high PAE high power using ultrathin Al-rich barrier GaN devices. IEEE, 2015.
[6] Zimmermann, T, et al. AlN/GaN Insulated-Gate HEMTs With 2.3 A/mm Output Current and 480 mS/mm Transconductance [J]. *IEEE Electron Device Letters* 29.**7**(2008):661-664.
[7] Koehler A. D, Nepal N, *et al*. Atomic Layer Epitaxy AlN for Enhanced AlGaN/GaN HEMT Passivation [J]. *Electron Device Letters*, IEEE, 34. **9**(2013):1115-1117
[8] Hua M, Lu Y, Liu S, *et al*. Compatibility of AlN/SiNx Passivation With LPCVD-SiNx Gate Dielectric in GaN-Based MIS-HEMT [J]. *IEEE Electron Device Letters*, 2016, **37**(3):265-268.
[9] Taking S, Khokhar A, Macfarlane D, *et al*. New Process for Low Sheet and Ohmic Contact Resistance of AlN/GaN MOS-HEMTs [J]. 2010. European Microwave Week 2010: Connecting the World, EuMIC 2010 - Conference Proceedings (2010) **306**-309
[10] Al-Khalidi A, Khalid A, Wasige E. AlN/GaN HEMT technology with in-situ SiNx passivation [C]// 2015 11th Conference on Ph. D. Research in Microelectronics and Electronics (PRIME). IEEE, 2015. pp251-253
[11] Yang S , Tang Z, Wong K Y, *et al*. Mapping of interface traps in high-performance Al_2O_3/AlGaN/GaN MIS-heterostructures using frequency- and temperature-dependent C-V techniques [C]// IEEE International Electron Devices Meeting 2013. pp.631-634
[12] Yang S, Liu S, Lu Y, *et al*. Interface Trap Analysis in GaN-Based Buried-Channel MIS-HEMTs [J]. *IEEE Transactions on Electron Devices*, 2015, **62**(6):1870-1878.
[13] Mizue C, Hori Y, Miczek M, *et al*. Capacitance? Voltage Characteristics of Al2O3/AlGaN/GaN Structures and State Density Distribution at Al2O3/AlGaN Interface [J]. *Japanese Journal of Applied Physics*, 2011, **50**(2):021001-021001-7.
[14] M, Capriotti, P, et al. Modeling small-signal response of GaN-based metal-insulator-semiconductor high electron mobility transistor gate stack in spill-over regime: Effect of barrier resistance and interface states[J]. *Journal of Applied Physics*, 2015, **117**(2):24506-24506.
[15] Ramanan N, Lee B, Misra V. Comparison of Methods for Accurate Characterization of Interface Traps in GaN MOS-HFET Devices [J]. *IEEE Transactions on Electron Devices*, 2015, **62**(2):546-553.
[16] Zhang Y, Huang S, Wei K, *et al*. Millimeter-Wave AlGaN/GaN HEMTs with 43.6% Power-Added-Efficiency at 40 GHz Fabricated by Atomic Layer Etching Gate Recess [J]. *IEEE Electron Device Letters*, 2020, PP(99):1-1.